Discussion

It is known that the pyrolysis of $Os_3(CO)_{10}(\mu\text{-SPh})(\mu\text{-H})$, in the absence of solvent at 200 °C, results in the elimination of benzene and the formation of a variety of higher nuclearity sulfido osmium carbonyl cluster compounds.[18] It was hoped that benzene elimination from **1** would lead to higher nuclearity clusters that contain carbene ligands.

The results of this study are summarized in Figure 3. The formation of compounds **2** and **5** confirms the loss of a phenyl group (benzene formation was not established), but no products containing carbene ligands were obtained. Compounds **3–5** each contain a bridging (dimethylamino)carbyne ligand. It is believed that the carbyne ligand was formed by an α-activation of the C–H bond of the carbene ligand. This transformation has been observed in the pyrolysis of **1** in solutions.[12] The formation of compounds **2–4** has involved a variety of ligand eliminations from **1**, presumably by competing reactions. Mechanistic details are not available at this time. Compound **5** is the only higher nuclearity product that was characterized, although it is suspected that red **6** is also a higher nuclearity species. Compound **5** is electron-precise and has adopted a cluster shape that is analogous to that of compound **11**. The mechanism of the formation of **5** is not clear at this time, but it seems that it could have been formed by a combination of **4** with an SOs_3 species.

The synthesis of high nuclearity carbene clusters is proving to be a great challenge. There is, to date, only one report of carbene-containing clusters in which the metal nuclearity is higher than three.[10] The high reactivity of carbene ligands on transition-metal clusters, and their propensity for transformation to carbyne ligands, as described in this report and previously, may be a major impediment in their synthesis.

Acknowledgment. These studies were supported by the Office of Basic Energy Sciences of the U.S. Department of Energy. We wish to thank Johnson-Matthey Inc. for a loan of osmium tetraoxide. The Brüker AM-300 NMR spectrometer was purchased with funds from the National Science Foundation under Grant CHE-8411172.

Registry No. **1**, 106499-78-9; **2**, 38979-82-7; **3**, 63373-87-5; **4**, 109637-86-7; **5**, 109669-11-6.

Supplementary Material Available: Tables of anisotropic thermal parameters and positional parameters for compounds **4** and **5** (6 pages); listings of observed and calculated structor factor amplitudes for **4** and **5** (46 pages). Ordering information is given on any current masthead page.

(18) Adams, R. D.; Horváth, I. T.; Mathur, P.; Segmüller, B. E.; Yang, L. W. *Organometallics* **1983**, *2*, 1078.

Coordination Chemistry of Methyl Iodide

Mark J. Burk, Brigitte Segmuller, and Robert H. Crabtree*

Sterling Chemistry Laboratory, Yale University, New Haven, Connecticut 06520

Received April 27, 1987

The complex $[IrH_2(IMe)_2(PPh_3)_2]SbF_6$ (**1**) contains two iodomethane groups coordinated via the iodine atoms. The Ir–I–C angles are 105.5 (4) and 108.2 (5)°. The coordinated iodomethane is activated toward nucleophilic attack at the carbon atom by NEt_3, the rate of which is enhanced by 10^4–10^5-fold relative to free MeI. Removing the hydride ligands with t-BuCH=CH_2 leads to oxidative addition to give $[MeIr(\mu\text{-I})(PPh_3)_2]_2$ (**2**). Crystal structures of **1** and **2** were determined.

Introduction

Main-group alkyls QR_n (Q = element of groups 15–17), such as PMe_3, SMe_2, and IMe, can in principle bind to a transition metal either with oxidative addition of the Q–C bond to the metal (eq 1) or via a lone pair on Q (eq 2).

$$R_nQ + ML_n \longrightarrow R_{n-1}Q(R)\text{—}ML_n \quad (1)$$

$$R_nQ + ML_n \rightarrow R_nQ{:}\rightarrow ML_n \quad (2)$$

The tendency to oxidative addition rises as $PMe_3 < SMe_2 < IMe$, and examples involving P–C cleavage in phosphines are rather rare. On the other hand, the tendency to bind via a lone pair falls as $PMe_3 > SMe_2 > IMe$, and no crystallographically authenticated example of an iodocarbon complex was known until our first report[1] in this area some years ago.

The origin of the trend found for oxidative addition may lie in the progressive lowering of the Q–C σ^* level as Q goes from P to I. As this happens, oxidative addition, either by attack of the metal at the Q–C σ^* or by single electron transfer into the Q–C σ^*, becomes easier. The trend in binding via Q is probably a result of the decreasing basicity of the lone pair(s) on Q as we go from P to I.

An earlier report[2] of the existence of an iodomethane complex was not confirmed[3] by a crystallographic study. We therefore felt we should determine the crystal structure of our complex. We and others have also reported cases of bromo–,[4] chloro–,[4a,5] and fluorocarbon[6] binding to transition metals, and even I_2 is now known to bind.[7]

(1) Crabtree, R. H.; Faller, J. W. Mellea, M. F.; Quirk, J. M. *Organometallics* **1982**, *1*, 1361–66.

(2) Lawson, D. N.; Osborn, J. A.; Wilkinson, G. W. *J. Chem. Soc. A* **1966**, 1733.

(3) (a) Troughton, P. G. H.; Skapski, A. *Chem. Commun.* **1968**, 575–6. Skapski, A. personal communication, 1985. Siedle A. R.; Newmark, R. A.; Pignolet, L. H. *Organometallics* **1984**, *3*, 855–9.

(4) (a) Burk, M. J.; Crabtree, R. H.; Holt, E. M. *Organometallics* **1984**, *3*, 638–40. (b) Barcelo, F.; Lahuerta, P.; Ubeda, M. A.; Foces-Foces, C.; Cano, F. H.; Martinez-Ripoll, M. *J. Chem. Soc., Chem. Commun.* **1985**, 43.

(5) Beck, W.; Schloter, K. *Z. Naturforsch., B: Anorg. Chem., Org. Chem.* **1978**, *33B*, 1214; **1980**, *35B*, 985.

(6) Kulawiec, R. J.; Holt, E. M.; Lavin, M.; Crabtree, R. H. *Inorg. Chem.* **1987**, *26*, 2559. Catala, R. M.; Cruz-Garritz, D.; Hills, A.; Hughes, D. L.; Richards, R. L.; Susa, P.; Torrens, H. *J. Chem. Soc., Chem. Commun.* **1987**, 261. Rust, P. M.; Stallings, W. C.; Monti, C. T.; Preston, R. K.; Glusker, J. P. *J. Am. Chem. Soc.* **1983**, *103*, 3206. Uson, R.; Fornies, J.; Tomas, M.; Cotton, F. A.; Falvello, L. R. *J. Am. Chem. Soc.* **1984**, *106*, 2482.

0276-7333/87/2306-2241$01.50/0

Table I. Crystallographic Data from X-ray Diffraction Studies

	$IrI_2P_2C_{38}H_{38}SbF_6$	$Ir_2I_2P_4C_{72}H_{66}2(SbF_6)\cdot{}^4/_3(CH_2Cl_2)$
	(A) Crystal Data	
temp, ±5 °C	23	24
space group	*Pbca*, No. 61	P$\bar{1}$, No. 2
a, Å	22.896 (6)	11.360 (2)
b, Å	19.307 (3)	12.843 (2)
c, Å	18.529 (5)	15.359 (3)
α, deg	90.0	106.71 (1)
β, deg	90.0	106.91 (2)
γ, deg	90.0	95.54 (1)
V, Å^3	1891 (6)	2013 (2)
M_r	1238.4	2358.8
Z	8	1
ρ_{calcd}, g/cm^3	2.008	1.946
	(B) Measurement of Intensity Data	
radiatn	Mo K*α* (0.71073 Å)	Mo K*α* (0.71073 Å)
monochromator	graphite	graphite
detector aperture (mm)		
horizontal ($A + B$ tan θ)		
A	3.0	3.0
B	1.0	1.0
vertical	4.0	4.0
cryst faces	0$\bar{1}$0, 101, 100, $\bar{1}$00, 0$\bar{1}\bar{1}$, $\bar{2}\bar{1}$0, 00$\bar{1}$, 001	001, 00$\bar{1}$, 100, $\bar{1}$01, 0$\bar{1}$1, 01$\bar{1}$, $\bar{1}$00
cryst size	0.41 mm × 0.19 mm × 0.39 mm	0.14 mm × 0.19 mm × 0.07 mm
crystl orientatn directn; deg from ϕ axis	normal to 00$\bar{1}$; 6.4°	normal to 0$\bar{2}$1; 6.9°
reflectns measd	*h*,*k*,*l*	*h*,±*k*,±*l*
max 2*θ*, deg	40	46
scan type	moving crystal–stationary counter	moving crystal–stationary counter
ω-scan width (A + 0.347 tan θ)°, *A* =	0.95	1.00
background	$^1/_4$ additional scan at each end of scan	$^1/_4$ additional scan at each end of scan
ω-scan rate (variable)		
max, deg/min	10	10
min, deg/min	1.7	1.5
no. of reflectns measd	4240	5566
data used ($F^2 > 3.0\ \sigma(F)^2$)	2335	3443
	(C) Treatment of Data	
absorption correctn coeff, cm^{-1}	55.195	49.898
grid	12 × 6 × 12	14 × 22 × 6
transmissn coeff		
max	0.3678	0.7555
min	0.1250	0.5080
P factor	0.010	0.010
final residuals		
R	0.040	0.046
R_w	0.042	0.048
esd of unit weight observn	2.693	2.482
largest shift/error value on final cycle	0.01	0.02
largest peak in final diff Fourier, e/Å^3	0.750	1.5

Although we reported an iodocarbon complex,[1] $[IrH_2(C_6H_4I_2)(PPh_3)_2]BF_4$, in 1982, we were only able to make what we believed to be the analogous MeI complex in poor yield, and no crystals of crystallographic quality could be grown of the fluoroborate salt. We now report a high-yield synthesis of the hexafluoroantimoniate salt, which has allowed us to determine the structure. We have also studied the chemistry of the new complex. Nucleophilic attack at the iodomethane carbon is greatly enhanced by binding, and oxidative addition of the ligand is induced by the loss of H_2 from the complex.

Table II. Selected Distances (Å) and Angles (deg)

	1	2
	Bond Distances	
Ir–I(1)	2.744 (1)	2.720 (1)
Ir–I(2)	2.781 (1)	2.697 (1)
Ir–P(1)	2.314 (3)	2.316 (3)
Ir–P(2)	2.311 (3)	2.302 (3)
I(1)–C(1)	2.13 (1)	
I(2)–C(2)	2.12 (2)	
Ir–C(1)	3.89 (2)	2.09 (1)
Ir–C(2)	3.99 (2)	
Ir–Ir		4.150 (1)
	Bond Angles	
I(1)–Ir–I(2)	87.98 (3)	80.14 (3)
I(1)–Ir–P(1)	95.73 (8)	
I(1)–Ir–P(2)	102.64 (8)	
I(2)–Ir–P(1)	97.58 (9)	
I(2)–Ir–P(2)	97.39 (8)	
P(1)–Ir–P(2)	156.6 (1)	100.5 (1)
Ir–I(1)–C(1)	105.5 (4)	
Ir–I(2)–C(2)	108.2 (5)	
Ir–I–Ir		99.86 (3)
P(1)–Ir–C(1)		100.2 (3)
P(2)–Ir–C(1)		91.8 (3)

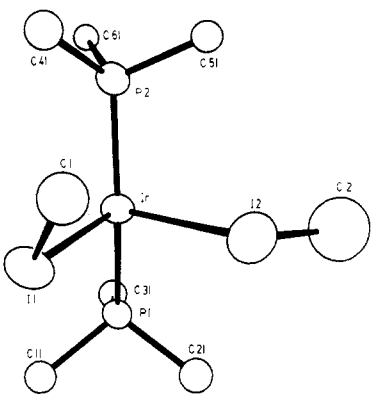

Figure 1. An ORTEP diagram of the $[IrH_2(IMe)_2(PPh_3)_2]^+$ cation of 1.

Results and Discussion

Synthesis of the MeI Complex. On hydrogenation in CH_2Cl_2, [Ir(cod)L_2]A loses cyclooctane and in the presence of MeI gives $[IrH_2(MeI)_2L_2]A$ (1). The product can be obtained in high yield by precipitation with Et_2O only when A is SbF_6. We have found this anion to be very useful. It gives crystalline derivatives as easily as does ClO_4^- but without the detonation hazard of the latter. It also appears to be less coordinating than ClO_4^-, BF_4^-, or PF_6^- and less subject to F^- loss than BF_4^-.

The Structure of the Methyl Iodide Complex. Crystallographic analysis of the compound (see Experimental Section and Tables I–IV and S1–3 in the supplementary material) show that this is an authentic iodomethane complex. The key feature of the discrete cation

(7) Van Beck, J. A. M.; Van Koten, G. Smeets, W. J. J.; Spek, A. L. *J. Am. Chem. Soc.* **1986**, *108*, 5010–11.

(8) Bellou, P. L.; Demartin, E.; Manassero, M.; Sansomi, M.; Caglio, G. *J. Organomet. Chem.* **1978**, *157*, 209.

Table III. Positional and Thermal Parameters and Their Estimated Standard Deviations for 1

atom	*x*	*y*	*z*	*B*(1,1)	*B*(2,2)	*B*(3,3)	*B*(1,2)	*B*(1,3)	*B*(2,3)	B_{eq}, Å^2
Ir	0.15644 (3)	0.18585 (4)	0.00343 (4)	2.32 (2)	2.62 (3)	3.04 (3)	−0.03 (4)	−0.00 (4)	−0.23 (4)	2.66 (1)
I(1)	0.15068 (5)	0.04888 (7)	0.04238 (8)	4.15 (6)	2.74 (6)	6.10 (7)	−0.15 (7)	0.46 (6)	−0.04 (7)	4.33 (3)
I(2)	0.16554 (6)	0.14267 (10)	−0.13932 (8)	5.97 (7)	7.4 (1)	5.47 (8)	0.18 (9)	−0.10 (7)	−1.08 (8)	6.29 (4)
Sb	0.14710 (5)	0.04475 (7)	0.33242 (7)	4.45 (6)	3.56 (7)	3.86 (6)	−0.27 (7)	0.35 (6)	−0.18 (7)	3.95 (3)
P(1)	0.0566 (2)	0.2046 (2)	0.0049 (3)	2.5 (2)	2.6 (3)	2.8 (2)	−0.2 (2)	0.1 (2)	0.1 (3)	2.6 (1)
P(2)	0.2539 (2)	0.2119 (3)	0.0212 (2)	2.6 (2)	2.7 (3)	2.9 (3)	0.2 (2)	0.4 (2)	−0.3 (2)	2.7 (1)

atom	*x*	*y*	*z*	*B*,Å^2	atom	*x*	*y*	*z*	*B*,Å^2
F(1)	0.1397 (4)	−0.0123 (6)	0.4127 (6)	5.9 (3)	C(33)	0.0555 (8)	0.4161 (11)	0.0377 (11)	5.1 (5)
F(2)	0.1768 (5)	0.1131 (7)	0.3922 (7)	7.5 (3)	C(34)	0.0052 (7)	0.4232 (10)	0.0771 (10)	4.3 (5)
F(3)	0.1559 (5)	0.0994 (8)	0.2518 (7)	9.3 (4)	C(35)	−0.0293 (7)	0.3696 (10)	0.0940 (9)	3.4 (4)
F(4)	0.1166 (5)	−0.0240 (7)	0.2729 (7)	8.0 (4)	C(36)	−0.0133 (6)	0.3033 (9)	0.0765 (9)	2.8 (4)
F(5)	0.0715 (5)	0.0778 (7)	0.3471 (6)	6.4 (3)	C(41)	0.3002 (7)	0.1537 (10)	0.0711 (10)	3.6 (4)
F(6)	0.2221 (4)	0.0108 (7)	0.3181 (6)	6.9 (3)	C(42)	0.2783 (6)	0.1190 (9)	0.1349 (9)	3.0 (4)
C(1)	0.2255 (8)	0.0015 (12)	−0.0048 (11)	5.4 (5)	C(43)	0.3126 (7)	0.0759 (10)	0.1731 (10)	4.0 (5)
C(2)	0.1514 (11)	0.2298 (15)	−0.2069 (15)	10.2 (8)	C(44)	0.3680 (8)	0.0617 (11)	0.1520 (10)	5.0 (5)
C(11)	0.0136 (6)	0.1474 (9)	0.0667 (9)	2.8 (4)	C(45)	0.3918 (8)	0.0917 (10)	0.0930 (10)	4.3 (5)
C(12)	0.0368 (7)	0.1344 (10)	0.1333 (10)	3.8 (4)	C(46)	0.3584 (7)	0.1370 (10)	0.0503 (10)	3.7 (4)
C(13)	0.0059 (8)	0.0918 (11)	0.1813 (11)	4.8 (5)	C(51)	0.2916 (6)	0.2312 (9)	−0.0640 (9)	2.4 (4)
C(14)	−0.0460 (8)	0.0661 (12)	0.1604 (11)	5.9 (6)	C(52)	0.3107 (7)	0.1786 (10)	−0.1081 (9)	3.5 (4)
C(15)	−0.0704 (8)	0.0801 (12)	0.0964 (11)	5.6 (5)	C(53)	0.3306 (7)	0.1941 (10)	−0.1749 (10)	4.5 (5)
C(16)	−0.0396 (7)	0.1228 (11)	0.0462 (11)	4.7 (5)	C(54)	0.3312 (8)	0.2590 (12)	−0.2003 (11)	5.4 (5)
C(21)	0.0180 (7)	0.1962 (10)	−0.0827 (9)	3.2 (4)	C(55)	0.311 (9)	0.3071 (12)	−0.1574 (11)	6.2 (6)
C(22)	0.0010 (7)	0.2555 (11)	−0.1181 (11)	4.2 (4)	C(56)	0.2919 (7)	0.2971 (10)	−0.0878 (90)	3.9 (5)
C(23)	−0.0240 (8)	0.2478 (13)	−0.1872 (12)	6.2 (5)	C(61)	0.2640 (6)	0.2898 (8)	0.0760 (8)	1.8 (4)
C(24)	−0.0277 (8)	0.1832 (12)	−0.2170 (11)	6.1 (6)	C(62)	0.2820 (7)	0.3287 (10)	0.1007 (9)	3.7 (4)
C(25)	−0.0101 (8)	0.1295 (11)	−0.1822 (11)	5.1 (5)	C(63)	0.2287 (7)	0.3864 (11)	0.1443 (10)	4.7 (5)
C(26)	0.0140 (7)	0.1328 (11)	−0.1156 (10)	4.5 (5)	C(64)	0.2832 (7)	0.4100 (10)	0.1583 (9)	4.0 (5)
C(31)	0.0375 (6)	0.2896 (9)	0.0366 (9)	2.7 (4)	C(65)	0.3280 (7)	0.3712 (11)	0.1322 (11)	4.9 (5)
C(32)	0.0718 (7)	0.3486 (10)	0.0166 (10)	4.3 (5)	C(66)	0.3207 (7)	0.3081 (10)	0.0917 (9)	3.6 (4)

Table IV. Positional and Thermal Parameters and Their Estimated Standard Deviations for 2[a]

atom	*x*	*y*	*z*	*B*(1,1)	*B*(2,2)	*B*(3,3)	*B*(1,2)	*B*(1,3)	*B*(2,3)	B_{eq}, Å^2
Ir	0.12218 (6)	0.09762 (5)	0.13507 (5)	2.43 (2)	1.96 (2)	2.52 (2)	0.30 (2)	0.36 (2)	0.52 (2)	2.47 (1)
I	0.0725 (1)	−0.11199 (8)	0.00871 (8)	3.87 (5)	2.44 (4)	3.49 (5)	0.95 (4)	−0.55 (4)	0.15 (4)	3.84 (3)
Sb	0.7807 (1)	0.7775 (1)	0.2239 (1)	6.52 (7)	6.06 (6)	7.41 (7)	1.37 (6)	2.98 (5)	3.43 (5)	6.23 (4)
P(1)	0.3050 (4)	0.0564 (3)	0.2213 (3)	2.7 (2)	2.9 (2)	2.8 (2)	0.5 (1)	0.4 (1)	0.8 (1)	2.9 (1)
P(2)	0.1490 (4)	0.2828 (3)	0.2202 (3)	3.6 (2)	2.3 (2)	2.5 (2)	0.3 (1)	0.8 (1)	0.4 (1)	3.0 (1)

atom	*x*	*y*	*z*	*B*, Å^2	atom	*x*	*y*	*z*	*B*, Å^2
F(1)	0.639 (1)	0.677 (1)	0.1295 (9)	11.1 (4)	C(34)	0.528 (2)	0.249 (2)	0.5409 (14)	7.1 (5)
F(2)	0.857 (2)	0.757 (1)	0.1339 (12)	15.3 (6)	C(35)	0.533 (2)	0.298 (2)	0.4726 (14)	7.6 (6)
F(3)	0.924 (1)	0.876 (1)	0.3125 (10)	11.5 (4)	C(41)	0.165 (1)	0.331 (1)	0.3495 (10)	3.6 (4)
F(4)	0.704 (2)	0.796 (1)	0.3156 (12)	16.4 (6)	C(42)	0.184 (1)	0.263 (1)	0.4056 (11)	4.5 (4)
F(5)	0.84 (2)	0.669 (2)	0.2674 (14)	18.4 (7)	C(43)	0.198 (2)	0.301 (1)	0.5043 (12)	5.7 (5)
F(6)	0.725 (2)	0.893 (1)	0.1948 (12)	15.4 (6)	C(44)	0.186 (2)	0.411 (2)	0.5390 (13)	6.4 (5)
C(1)	0.001 (1)	0.053 (1)	0.2033 (11)	4.4 (4)	C(45)	0.166 (2)	0.484 (2)	0.4878 (13)	6.9 (5)
C(11)	0.292 (1)	−0.089 (1)	0.2147 (10)	2.9 (3)	C(46)	0.160 (2)	0.446 (1)	0.3878 (12)	5.7 (5)
C(12)	0.375 (1)	−0.153 (1)	0.1794 (11)	4.3 (4)	C(51)	0.014 (1)	0.345 (1)	0.1737 (10)	3.5 (3)
C(13)	0.360 (2)	−0.266 (1)	0.1735 (12)	5.5 (5)	C(52)	−0.088 (1)	0.328 (1)	0.2028 (11)	4.4 (4)
C(14)	0.266 (1)	−0.316 (1)	0.1972 (12)	4.9 (4)	C(53)	−0.197 (2)	0.372 (2)	0.1691 (13)	6.0 (5)
C(15)	0.185 (2)	−0.253 (1)	0.2283 (12)	5.3 (4)	C(54)	−0.191 (2)	0.433 (2)	0.1073 (13)	6.7 (5)
C(16)	0.197 (1)	−0.138 (1)	0.2362 (11)	4.3 (4)	C(55)	−0.094 (2)	0.449 (2)	0.0766 (14)	7.1 (5)
C(21)	0.416 (1)	0.086 (1)	0.1635 (9)	2.9 (3)	C(56)	0.018 (2)	0.405 (1)	0.1114 (12)	5.3 (4)
C(22)	0.548 (1)	0.090 (1)	0.2028 (11)	4.9 (4)	C(61)	0.285 (1)	0.364 (1)	0.2092 (10)	3.5 (3)
C(23)	0.627 (2)	0.116 (1)	0.1548 (12)	5.9 (5)	C(62)	0.286 (1)	0.346 (1)	0.1136 (11)	4.5 (4)
C(24)	0.581 (2)	0.139 (1)	0.0708 (12)	5.4 (4)	C(63)	0.392 (2)	0.409 (1)	0.1043 (12)	5.7 (5)
C(25)	0.451 (1)	0.137 (1)	0.0293 (12)	5.1 (4)	C(64)	0.483 (2)	0.477 (1)	0.1879 (13)	5.9 (5)
C(26)	0.368 (1)	0.108 (1)	0.0755 (11)	4.1 (4)	C(65)	0.481 (2)	0.497 (1)	0.2774 (12)	5.6 (5)
C(31)	0.395 (1)	0.129 (1)	0.3490 (10)	3.5 (3)	C(66)	0.378 (1)	0.440 (1)	0.2941 (11)	4.4 (4)
C(32)	0.385 (1)	0.080 (1)	0.4179 (11)	4.8 (4)	Cl(1)	0.5809 (8)	0.2105 (7)	0.4001 (6)	8.1 (2)
C(33)	0.455 (2)	0.145 (2)	0.5185 (14)	7.8 (6)	Cl(2)	0.7912 (15)	0.0815 (14)	0.4924 (12)	19.3 (6)
C(1S)	0.896 (3)	0.135 (3)	0.460 (2)	9 (1)					

[a] The form of the anisotropic thermal parameter is $\exp[-^1/_4(h^2a^{*2}B(1,1) + k^2b_2B(2,2) + l^2c^{*2}B(3,3) + 2hka^*b^*B(1,2) + 2hla^*cB(1,3) + 2klb^*c^*B(2,3))]$. Estimated standard deviations in the least significant digits are shown in parentheses.

(Figure 1) is the coordination of two MeI ligands via iodine. The Ir–I bond lengths of 2.744 (1) and 2.781 (1) Å are slightly longer than in the analogous *o*-$C_6H_4I_2$ compound (2.745 (1) and 2.726 (2) Å) but within the range of Ir–I distances known[8] for I^- complexes, e.g., 2.786 Å in [Ir(ArN_2H)HI(PPh_3)$_2$]. A single coordinate bond is clearly present. The angles at I, 105.5 (4) and 108.2 (5)°, are particularly interesting. The $C_6H_4I_2$ complex had slightly smaller angles (99.9 (5) and 101.8 (5)°), but extra constraints are present in a chelate ring. In both cases, not only are the angles less than tetrahedral but also the iodocarbon incurs greater steric hindrance by adopting a conformation that leads to a smaller Ir–I–C angle. The coordination around I therefore shows a strong nonlinear preference. These results broadly confirm the recent prediction by Hoffman et al.[9] that the Pt–I–C bond angle

in the hypothetical compound $Ph(NH_3)_2Pt(IMe)^+$ would be 100° (experimental value for 1: 106.9° (av)). The M–I–C angle (θ) adopted arises from the hybridization of the lone pairs on I. There are three, one of sp-type (coordination to which would give θ = 180°) and two predominantly p-type (θ = 90°). Of the two, the p-type HOMO lone pairs are the higher in energy by about 1.5 eV (as expected in view of the ca. 50% s character of the sp-type lone pair) so this orbital is employed in bonding to the metal. The fact that the observed values of θ are 10–18° greater than 90° may be accounted for by partial rehybridization to include some s character in the lone pair and by steric effects.

If this explanation is true, then the structures of R_2Te and RTe complexes should show similar bond angles. $[Pd(SCN)_2(TeR_2)_2]$ (R = $(CH_2)_3SiMe_3$) has M–Te–C angles of 101.6 (3)[10] and 102.3 (3)°, and $(C_7H_7)Mo(CO)_2(TePh)$ has an angle of 105°.[11] The tellurium therefore seems to coordinate using orbitals having much greater p character than sp^3. M–S–C angles in unhindered alkanethiolate complexes are much the same, 102° in $[N(n\text{-}Pr)_4][Fe(SEt)_4]$ and 104° in $[NEt_4][Fe(SMe)_4]$, for example.[12] Complexes of SR_2 tend to have higher bond angles than do those of TeR_2, e.g., 103.3 (2)° in $[CuCl_2(n\text{-}BuS(CH_2)_2S\text{-}n\text{-}Bu)]_2$,[13] perhaps due to the greater ease of hybridization in the lower elements of the group, and the shorter M–S distances, leading to higher steric repulsions. In contrast $M(QR_3)$ complexes (Q = P, As, Sb, Bi; R = Me or Ph) have M–Q–C angles *larger* than the tetrahedral, e.g., from 115.6° for P to 118.9° for Bi in the series of complexes: $[Cr(CO)_5(QR_3)]$.[14] While TeR_2 and IMe bind via largely p character lone pairs, QR_3 has used all its predominantly p-type orbitals in bond formation to R, leaving the remaining largely s-type orbital as the lone pair. Since the C–Q–C angles are less than tetrahedral, as expected for predominantly p-type orbitals (e.g., 102.6° for P to 98.7° for Bi in $[Cr(CO)_5(QPh_3)]$), the average M–Q–C angles must exceed 109°.

In the series SbR_3, TeR_2, and IR, several factors favor decreasing basicity, the electronegativity of the elements rises significantly (Sb, 1.9; Te, 2.1; I, 2.5), and the number of donor alkyl groups falls, yet the second and third members of the series are still capable of acting as ligands. This may be due to the switch in lone-pair character, from largely s (less basic) to largely p (more basic) that takes place on moving from group 15 to groups 16 and 17.

In principle, the MeI can act as a π-acceptor. Probably not via its vacant d orbitals but more likely via the LUMO, the vacant σ^* orbital.[15] This extends along the C–I vector away from the bond in both directions. As carbon is the more electronegative element, the σ^* orbital has more I than C character. The bent conformation permits overlap of the lobe of the σ^* based on I with metal d orbitals, and the two MeI's even adopt conformations in which each σ^* orbital is aligned with different d orbitals on the metal. C(2)–I(2) is very close to the Ir–I(1)–I(2) plane, and C(1)–I(1) is only about 28° out of alignment with the I(1)–P(1)–P(2) plane. An orientation of C(1)–I(1) which made it coplanar with the I(1)–P(1)–P(2) plane would be opposed by the steric effects of the PPh_3 groups and by lone pair–lone pair repulsions between the iodines. The extent of the proposed σ^*–d interaction is unclear, but the position of the σ^* level of free MeI (–5 eV) is not very different[16] from that of the π^* levels in free CO (–6 eV); CO, of course, has long been known to be a good π-acceptor ligand.[17] Any occupation of the C–I σ^* by metal electrons does not lengthen the C–I bond relative to free MeI because (as happens[15b] with PR_3) binding removes lone-pair electron density on I and so leads to a shortening of the C–I bond (free MeI = 2.1387 Å[15c]) by reducing I(lp)–CH_3 repulsions.

Electrophilic Activation of the C–I Bond. Silver and mercuric ions are well-known to activate alkyl halides for solvolysis.[18] BF_3 and $AlCl_3$ are used as halide acceptors in Friedel–Crafts reactions involving alkyl and acyl halides. Kinetic evidence for adduct formation has been obtained in some cases although controversy has sometimes arisen over whether the adducts are molecular (e.g., $RX\,AlX_3$) or are ion pairs ($R^+\,AlX_4^-$). Adducts have occasionally been isolated at low temperature, e.g., i-PrCl·BF_3 at –110 °C, but have never been characterized crystallographically.[19]

We were interested to see whether our stable MeI complex showed activation of the C–I bond toward nucleophilic attack. Acetate ion reacted at room temperature but only with displacement of MeI to give $[IrH_2(OAc)(PPh_3)_2]$; pyridine behaved in an analogous way. NEt_3 did not displace MeI but gave 1 mol equiv of NEt_3Me^+/Ir. In parallel runs in CD_2Cl_2 at 25 °C, NEt_3 (0.12 M) reacted with free MeI (0.24 M) over 25 min but with $[IrH_2(MeI)_2(PPh_3)_2]BF_4$ (0.12 M) within the time that the first NMR data could be collected (30 s). The rate acceleration is therefore at least 50-fold. Along with the $[NMeEt_3]I$, 1 mol of free MeI was also observed by ^1H NMR. Apparently, the neutral iridium species that are formed in the reaction release the second MeI into the solution. The NMR spectrum shows that several hydride complexes are formed in the reaction. One of these (δ(Ir–*H*) –20.5 (J(P,H) = 16 Hz)) is also formed from KI and $[IrH_2(Me_2CO)_2(PPh_3)_2]SbF_6$ and is tentatively identified as $[IrH_2(\mu\text{-}I)(PPh_3)_2]_2$.

The $[NMeEt_3]I$ can be isolated directly from the reaction when it is run in $CHCl_3$ because the product precipitates under these conditions. The ^1H NMR of the salt was identical with that of an authentic sample[20] prepared by standard methods.

In order to get a quantitative idea of the rate acceleration, we tried to cool the reaction mixture so that the MeI complex might react at a rate convenient to measure by ^1H NMR. Even at –80 °C, the reaction was over before the first spectrum could be obtained. This implies that the rate acceleration on binding is on the order of 10^4–10^5.

This rate enhancement means that iodomethane complexes might be useful reagents in organic synthesis. In particular a chiral alkylating agent should in principle be possible, given a chiral Lewis acidic metal fragment. Adams et al.[21] showed that coordinating Me_3S^+ led to rate

(9) Ortiz, J. V.; Havlas, Z.; Hoffmann, R. *Helv. Chim. Acta* **1984**, *67*, 1.
(10) Gysling, H. R.; Luss, H. R.; Smith, D. L. *Inorg. Chem.* **1979**, *18*, 2696.
(11) Rettenmeier, A.; Weidenhammer, K.; Ziegler, M. L. *Z. Anorg. Allg. Chem.* **1981**, *173*, 91.
(12) Koch, S. J., personal communication, 1985.
(13) Cohen, R.; Ou, C. C.; Lalancette, R. A.; Borowski, W.; Potenza, J. A.; Schugar, H. J. *Inorg. Chem.* **1979**, *18*, 217.
(14) Carty, A. J.; Taylor, N. J.; Coleman, H. W.; Lappert, M. F. *J. Chem. Soc., Chem. Commun.* **1979**, 639.
(15) (a) Eisenstein, O., personal communication, 1985. Uehara, Y.; Saito, N.; Yonezawa T. *Chem. Lett.* **1973**, *2*, 495. (b) Orpen, A. G. *J. Chem. Soc., Chem. Commun.* **1985**, 1310. (c) Costain, C. C. *J. Chem. Phys.* **1958**, *18*, 1645.
(16) Sahni, R. C. *Trans. Faraday Soc.* **1953**, *49*, 1246. Scherr, C. W. *J. Chem. Phys.* **1955**, *23*, 569.
(17) Abel, E. W.; Stone, F. G. A. *Q. Rev. Chem. Soc.* **1969**, *23*, 325.
(18) Kevill, D. N. (Chapter 20); Dumas, J. M.; Gomel, M.; Guerin, M. (Chapter 21) In *Chemistry of the Functional Groups*; Suppl. D. Patai, S., Ed.; Wiley: Chichester, 1983; Suppl. D.
(19) Nakane, R.; Kurihara, O.; Natsubori, A. *J. Phys. Chem.* **1964**, *68*, 2876.
(20) Munz, R.; Gasser, A.; Simchen, G. *Justus Liebigs Ann. Chem.* **1978**, *12*, 1937–45.

enhancements of 10^2–10^3 in the alkylation of NEt_3.

Since we have an unusually bulky MeI equivalent reagent, we wondered whether stereoselective methylation might occur with a suitable substrate, such as *N*-methyl-4-*tert*-butylpiperidine. House[22] showed that this amine gives predominant axial methylation with CD_3OTs (ratio = 87:13). Unfortunately, the ratio is little changed when the CD_3I complex is employed (axial:equatorial ratio = 75:25).

We also examined the reaction of the complex with the more hindered amine $N(i\text{-}Pr)_2Et$ because the reaction with the free amine is inefficient (only a 50% yield of $[N(i\text{-}Pr)_2EtMe]I$ is obtained after 3 h under conditions analogous to those used above for NEt_3).[23] The origin of the methyl group was confirmed by showing that the CD_3I complex gives $[N(i\text{-}Pr)_2EtCD_3]I$. $N(i\text{-}Pr)_2(n\text{-pentyl})$ only reacted inefficiently with the MeI complex (ca. 20% yield of ammonium salt after 2 days).

Oxidative Addition in a Methyl Iodide Complex. In most metal complexes, MeI binding would probably lead to immediate oxidative addition. The reluctance to oxidatively add in this case probably arises from the fact that the metal in 1 is formally Ir(III), and Ir(III) to Ir(V) oxidative addition is probably rather unfavorable. To test this we synthesized some Ir(I) halocarbon complexes,[4a] $[Ir(cod)(Ph_2PC_6H_4X)]A$ (X = Br or Cl). These did not undergo oxidative addition either, even at 90 °C in CH_2Cl_2, until induced to do so by addition of H^- to the metal ($LiBEt_3H$/THF/25 °C/2 h or NaO_2CH/CH_2Cl_2/25 °C/44 h) (eq 3). The product complex arises from H abstraction

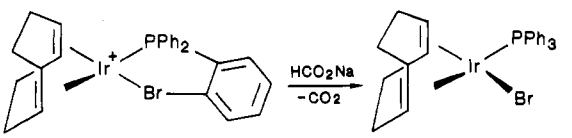

(3)

from the metal by the cyclometalated phosphine formed on oxidative addition.[24] This indicates that other factors also disfavored oxidative addition.

In spite of these results we attempted to induce oxidative addition by "reducing" the metal to Ir(I) by abstracting H_2 with our hydrogen acceptor reagent[25] *t*-BuCH=CH_2 (eq 4). This took place readily over 10 h at 20 °C to give

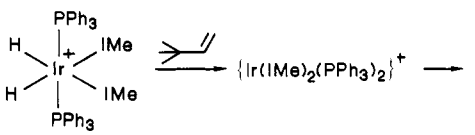

1

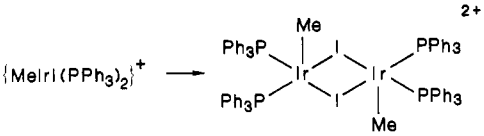

(4)

$[IrMe(PPh_3)_2(\mu\text{-}I)]_2A_2$ (**2**), an orange, crystalline complex formed in 60% yield. The product appears to be the dimer of the simple oxidative addition product "$IrMeI(PPh_3)_2$" and is only sparingly soluble in CH_2Cl_2.

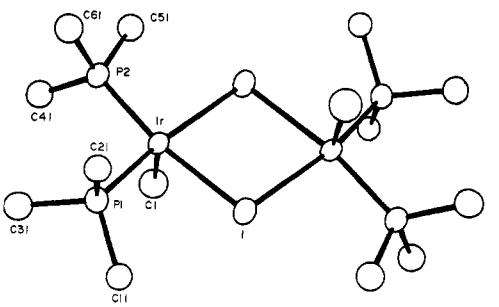

Figure 2. An ORTEP diagram of the $[Ir_2(\mu\text{-}I)_2Me_2(PPh_3)_4]^{2+}$ cation of **2**.

The ^1H NMR (CD_2Cl_2) shows a broad triplet at δ 3.56 ($^2J(P,H)$ = 1.9 Hz) for the Ir–Me groups, and the ^{31}P NMR, a resonance at −7.9 ppm (relative to external 85% H_3PO_4). In the ^{13}C NMR the IrMe group appears at −18.4 ppm, and the $^1J(C,H)$ of 139.1 Hz is normal.

Unfortunately we were not able to observe or characterize the proposed intermediate in this reaction: $\{Ir(IMe)_2(PPh_3)_2\}^+$.

The Structure of 2. In order to characterize the compound, we undertook an X-ray diffraction study (Tables I–IV and S1–3 (supplementary material)). Complex **2** is a dimer bridged via a planar $Ir(\mu\text{-}I)_2Ir$ ring, with an Ir···Ir distance (4.15 Å) which rules out an Ir–Ir bond (Figure 2). The inversion center in the molecule makes each half structurally identical. The coordination geometry is square-pyramidal, relatively rare for Ir(III), with a slight distortion in which P(1) bends away and P(2) bends toward the methyl group from their idealized positions. The Ir–I distances of 2.720 (1) and 2.697 (1) Å are typical for bridging iodo groups (cf. $[Cp^*IrI(\mu\text{-}I)]_2$, 2.710 Å).[26]

The structure[3] of $MeRhIr(PPh_3)_2$, formed from either $RhCl(PPh_3)_3$ or $Rh(PPh_3)_3^+$ and MeI and once believed to be a MeI complex, is comparable to that of **2**. The only important difference is that the two phosphines are trans and the geometry is slightly less distorted.

Other Iodocarbon Complexes. Analogous crystalline complexes of type **1** were prepared by the same route for PhI, EtI, *i*-PrI, and $C_6H_{11}I$ in 75–94% yields, but they were somewhat less thermally stable and satisfactory analyses were not obtained.

Unfortunately, attempts to observe alkylation reactions with NEt_3 at 25 °C led only to displacement of the halocarbon. The iodobenzene and iodoethane complexes reacted with *t*-BuCH=CH_2 to give species that we formulate as the phenyl and ethyl complexes of type **2**.

Mechanism of the Oxidative Addition. The usual pathways seem unlikely for this system. Nucleophilic attack at carbon is not usually observed for PhI and is unlikely for a cationic metal center such as we have here. Single electron transfer is not usually observed for MeI and is also unlikely for a cationic system. A more reasonable mechanism would be the direct migration of the alkyl or aryl group from the coordinated halocarbon to the metal. This possibility has been examined theoretically by Hoffman et al.[9]

Conclusion

We have shown that iodocarbon complexes bind in a bent R–I–M arrangement using a p-type lone pair on iodine. The binding activates iodomethane toward nucleophilic attack at carbon. We have also shown that oxidative addition can take place if the Ir is first reduced from Ir(III) to Ir(I).

(21) Adams, R. D.; Blankenship, C.; Segmuller, B. E.; Shiralian, M. *J. Am. Chem. Soc.* **1983**, *105*, 4319–26.
(22) House, H. O.; Tefertiller, B. A.; Pitt, C. G. *J. Org. Chem.* **1966**, *31*, 1073–79.
(23) Robinson, R. A. *J. Org. Chem.* **1951**, *16*, 1911–20.
(24) Burk, M. J. Ph.D. Thesis, Yale 1987. Burk, M. J.; Holt, E. M.; Crabtree, R. H. *J. Organomet. Chem.*, submitted for publication.
(25) Crabtree, R. H.; Mihelcic, J. M.; Quirk, J. M. *J. Am. Chem. Soc.* **1979**, *101*, 7738–9. Crabtree, R. H.; Mellea, M. F.; Mihelcic, J. M.; Quirk, J. M. *J. Am. Chem. Soc.* **1982**, *104*, 107–113.
(26) Churchill, M. R.; Julius, S. A. *Inorg. Chem.* **1979**, *18*, 1215–21.

Experimental Section

Syntheses were performed under purified N_2 or argon atmospheres by Schlenk techniques. NMR data [reported as δ (ppm), multiplicity (coupling constant, Hz), assignment] were recorded on Bruker WM500, HX490, and WM250 and JEOL FX-90Q (^1H), WM500 (^{13}C), and CFT-20 and WM500 (^1P) instruments. Phosphines were obtained from Strem Chemicals and other reagents from Aldrich Chemical Co. Iodocarbons were distilled and stored in the dark over Cu metal and under N_2.

Dihydridobis(triphenylphosphine)bis(iodomethane)iridium(III) Hexafluoroantimoniate (1). To $[Ir(cod)(PPh_3)_2]SbF_6$[27] (300 mg, 0.283 mol) in CH_2Cl_2 (0 °C, 8 mL) in the dark was added MeI (1 mL) under N_2. The N_2 was then replaced by a H_2 atmosphere and the mixture stirred for 30 min. While the H_2 atmosphere was maintained, Et_2O (50 mL) and pentane (20 mL) were added to precipitate the colorless product, which was filtered, washed with Et_2O, and dried in vacuo. The resulting white solid was immediately recrystallized from CH_2Cl_2 (5 mL) by the addition of Et_2O/pentane (2:1 v/v, 60 mL) to give colorless microcrystals. The product (305 mg, 85%) was filtered, washed with pentane, and dried in vacuo. ^1H NMR (CD_2Cl_2): −20.3, br, Ir–H; 1.55, s, MeI; 7.5, c, Ph. ^{31}P NMR (CH_2Cl_2): +10.7 ppm. ^{13}C NMR (CD_2Cl_2): −12, s, MeI; 126–136, c, PPh_3. The complex is spectroscopically very similar to the known[1] BF_4^- salt. The CD_3I complex was prepared in the same way from CD_3I. ^2H NMR (CH_2Cl_2): 1.60, s, CD_3I.

The other iodocarbon complexes were prepared by an analogous route. Yields: R = Ph, 94%; R = Et, 85%; R = *i*-Pr, 83%; R = Cy, 75%. The complexes did not give satisfactory combustion analyses probably because they lose halocarbon readily on heating. ^1H NMR (CD_2Cl_2): R = Ph, −21.4, br, Ir–H; 6.93, d (8), *o*-H; 7.01, t (8); *m*-H; 7.04, t (8), *p*-H; 7.4–7.5, PPh_3; R = Et, −20.25, 5 (14.6), Ir–H; 1.2, t (7.5), CH_3; 2.44, q (7.5), CH_2; 7.46–7.51, PPh_3; R = *i*-Pr, −20.2, 5 (br), Ir–H; 1.25, d (5.4), CH_3; 3.3, sept (5.4), CH; 7.46–7.5, PPh_3; R = Cy, −20.7, br, Ir–H (at −80 °C, −19.33, t (14.4)); 1.37, 1.43, c, Cy; 3.25, quint (br), axial C–H of Cy; 7.47–7.51, PPh_3.

Bis(μ-iodo)dimethyltetrakis(triphenylphosphine)diiridium(III) Bis(hexafluoroantimoniate) (2). $[IrH_2(MeI)_2(PPh_3)_2]SbF_6$ (1, 310 mg, 0.25 mmol) and *t*-BuCH=CH_2 (128 μL, 1 mmol) were stirred in CH_2Cl_2 (10 mL) for 10 h. Et_2O (40 mL) was added to the resulting orange solution to precipitate **2** as an orange solid. This was filtered, washed with Et_2O, and dried in vacuo. Recrystallization from CH_2Cl_2 (10 mL) by addition of Et_2O (40 mL) gave orange microcrystals (164 mg, 60%). ^1H NMR (CD_2Cl_2): 3.56, t (br, 1.9), Ir–Me; 7.25, c, PPh_3. $^1H\{^{31}P\}$ NMR (CD_2Cl_2): −7.9 ppm. $^1H\{^{13}C\}$ NMR (CD_2Cl_2): −18.4, br, s, Ir–Me; 127–134, PPh_3. ^{13}C NMR: −18.4, q (139), IrMe. Anal. Calcd for $C_{74}H_{66}I_2P_4Sb_2F_{12}Ir_2 \cdot 2CH_2Cl_2$: C, 38.70; H, 2.99; I, 10.76; F, 9.67. Found: C, 38.83; H, 3.16; I, 10.87; F, 9.46.

The phenyl and ethyl analogues were prepared in an analogous way but were not examined in detail. ^1H NMR: R = Ph, 7.1–7.5, c, Ph; R = Et, 1.64, t (7.1), CH_3; 4.74, q (7.1), CH_2. ^{13}C NMR: R = Ph, 103, br, ipso-C of Ph; 125–141, *o*-, *m*-, and *p*-C of Ph.

Crystallographic Analyses. Crystals of **1** and **2** suitable for X-ray diffraction measurements were grown by diffusing ether into a methylene chloride solution at 4 °C. A crystal of **1** was mounted in a thin-walled glass capillary tube under a nitrogen atmosphere. A crystal of **2** was mounted in a thin-walled glass capillary tube. Diffraction measurements were made on an Enraf-Nonius CAD-4 fully automated diffractometer. Unit cells were determined from using 25 randomly selected reflections. Crystal data and data collection parameters are listed in Table I. Data processing was performed on a PDP 11/45 using the Enraf-Nonius SDP program library (version 18) or a VAX 11/750 using the Enraf-Nonius SDP program library (VAX version 1). Absorption corrections of a Gaussian integration type were applied to the data of both structures. Full-matrix least-squares refinement minimized the function $\sum w(|F_o| - |F_c|)^2$, where $w = 1/\sigma(F)^2$, $\sigma(F) = \sigma(F_o^2)/2F_o$, and $\sigma(F_o^2) = [\sigma(I_{raw})^2 + (PF_o^2)^2]^{1/2}/Lp$.

For **1** the space group *Pbca* was determined from the observed systematic absences. The structure was solved by a combination of Patterson and difference Fourier techniques. The coordinates of the iridium atom were obtained from a three-dimensional Patterson map. The coordinates of all remaining atoms were obtained from a series of difference Fourier synthesis. The iridium, iodine, phosphorus, and antimony were refined with anisotropic thermal parameters. The fluorine and carbon atoms were refined with isotropic thermal parameters.

For **2** the space group $P\bar{1}$ was assumed and confirmed by the successful solution and refinement of the structure. The structure was solved by a combination of Patterson and difference Fourier techniques. The coordinates of the iridium atom obtained from a three-dimensional map. The coordinates of all remaining atoms were obtained from a series of difference Fourier syntheses. The methylene chloride was refined with $^2/_3$ occupancy. The thermal parameters for iridium, iodine, phosphorus, and antimony atoms were refined anisotropically. The carbon, chlorine, and fluorine atoms were refined with isotropic thermal parameters.

Estimated standard deviations for the bond distance and angle calculations were calculated by using the inverse matrix obtained on the final cycle of refinement. Tables of structure factor amplitudes are available for both structures; see supplementary material.

Acknowledgment. We thank the donors of the Petroleum Research Fund, administered by the American Chemical Society for funding, A. Skapski for unpublished data, and O. Eisenstein and J. Lauher for discussions.

Registry No. 1, 110169-78-3; 1 (CD_3I complex), 110077-59-3; 2, 110077-57-1; $[IrH_2(PhI)_2(PPh_3)_2]SbF_6$, 110169-80-7; $[IrH_2(EtI)_2(PPh_3)_2]SbF_6$, 110077-61-7; $[IrH_2(i\text{-}PrI)_2(PPh_3)_2]SbF_6$, 110077-63-9; $[IrH_2(CyI)_2(PPh_3)_2]SbF_6$, 110095-11-9; $[Ir_2(\mu\text{-}I)_2Ph_2(PPh_3)_4](SbF_6)_2$, 110077-65-1; $[Ir_2(\mu\text{-}I)_2Et_2(PPh_3)_4](SbF_6)_2$, 110077-70-8; $[IrH_2(OAc)(PPh_3)_2]$, 12103-82-1; $[IrH_2(py)(PPh_3)_2]^+$, 110077-66-2; $[IrH_2(MeI)_2(PPh_3)_2]BF_4$, 82582-66-9; $[IrH_2(\mu\text{-}I)_2(PPh_3)_2]_2$, 110077-67-3; $[IrH_2(Me_2CO)_2(PPh_3)_2]SbF_6$, 110077-68-4; $[NMeEt_3]I$, 994-29-6; $[N(i\text{-}Pr)_2EtCD_3]I$, 110046-21-4; $[N(i\text{-}Pr)_2(n\text{-pentyl})Me]I$, 110046-22-5; $[N(i\text{-}Pr)_2EtMe]I$, 68714-21-6; $[Ir(cod)(PPh_3)_2]SbF_6$, 91410-27-4; MeI, 74-88-4; *t*-BuCH=CH_2, 558-37-2; $N(i\text{-}Pr)_2Et$, 7087-68-5; $N(i\text{-}Pr)_2(n\text{-pentyl})$, 110046-20-3.

Supplementary Material Available: Tables of calculated H-atom positions (Table S2) and a full listing of angles and distances (4 pages); listings of observed and calculated structure factors (Table S1) (34 pages). Ordering information is given on any current, masthead page.

(27) Crabtree, R. H.; Parnell, C. P.; Uriarte, R. J. *Organometallics* **1987**, *6*, 696–99.